Defect Formation in Quench-Cooled Superfluid Phase Transition

V. M. Ruutu,[1] V. B. Eltsov,[1,*] M. Krusius,[1] Yu. G. Makhlin,[1,†] B. Plaçais,[2] and G. E. Volovik[1,†]

[1]*Low Temperature Laboratory, Helsinki University of Technology, Box 2200, FIN-02015 HUT, Finland*

[2]*Laboratoire de Physique de la Matière Condensée, E.N.S., CNRS URA 1437, F-75231 Paris Cédex 05, France*

(Received 7 April 1997)

We use neutron absorption in rotating ^{3}He-B to heat locally a ~100-μm-size volume into normal phase. When the heated region cools back in microseconds, vortex lines are formed. We record with NMR the number of lines vs the applied superflow velocity and compare to the Kibble-Zurek theory of vortex-loop freeze-out from a random network of defects. The measurements confirm the calculated loop-size distribution and indicate that the superfluid state itself forms as a patchwork of competing A- and B-phase blobs. The consequences to the $A \rightarrow B$ transition in supercooled ^{3}He-A are discussed. [S0031-9007(98)05361-7]

PACS numbers: 67.57.Fg, 05.70.Fh

A rapid phase transition generally leads to abundant disorder and inhomogeneity in a heterogeneous system. But even in the ideal homogeneous case, where extrinsic influence is absent, a phase transition far out of equilibrium might result in the formation of defects. This phenomenon, if shown to be true, could explain the change in the early Universe from an initial homogeneous state to that at present with large-scale structure [1]. However, reproducible measurements on the density and distribution of defects as a function of transition speed are experimentally a challenging task [2].

It was recently observed [3] that quantized vortices are created in superfluid ^{3}He-B in one of the fastest second order phase transitions probed to date. Here the transition is produced locally in a small volume, within the bulk medium far from boundaries, by irradiating ^{3}He-B superflow with ionizing radiation. The most practical heating effect is obtained from the absorption reaction of a thermal neutron, which creates a local overheating of suitable magnitude and volume. Vortices are then found to form in increasing number per absorption reaction as a function of the superflow velocity.

Homogeneous model.—There are several possible explanations to this phenomenon. We show that a quantitative comparison can be established with the theory of defect formation in a rapidly quenched second order phase transition which was proposed by Kibble [1] and Zurek [2]. In this time dependent transition the order parameter of the broken-symmetry phase begins to form independently in different spatially disconnected regions, by falling into the various degenerate minima of the Ginzburg-Landau free-energy functional. Superfluid coherence is then established only locally, in causally separated regions. These grow in size with time and form defects at their boundaries when they meet an adjacent region in a different free-energy minimum.

The expected domain size of the inhomogeneity, or the characteristic length scale in the initial random network of defects [2], is $\xi_v = \xi_0(\tau_Q/\tau_0)^{1/4}$. Here $\xi_0 \sim 20$ nm is the zero temperature superfluid coherence length, $\tau_0 \sim \xi_0/v_F \sim 1$ ns the order parameter relaxation time far below T_c, and v_F the Fermi velocity. The deviation from equilibrium is described by the cooling rate $\tau_Q = [T/|dT/dt|]_{T=T_c}$ at T_c, which in our ^{3}He-B experiment is $\tau_Q \sim 5$ μs. After the quench the defects relax, unless an external bias field is applied. In our case the superflow from rotation causes vortex loops to escape into the bulk liquid. There the rings expand to rectilinear vortex lines, which can then be counted with NMR. The bias for the preference between ^{3}He-A or ^{3}He-B can be controlled with the choice of pressure or magnetic field.

Initial inhomogeneity.—The Kibble-Zurek (KZ) mechanism has been demonstrated to produce random networks of defects in numerical simulations [4]. It has also been compared to experiments on liquid crystals [5] and superfluid ^{4}He II [6]. However, the KZ model describes an infinite and spatially homogeneous system while any laboratory sample is of finite size with nonzero gradients. In our ^{3}He-B experiment the superfluid transition moves through the rapidly cooling bubble as a phase front with a width $\sim[|\nabla T|/T]^{-1}_{T=T_c}$. A further important difference from the KZ model is the existence of the broken-symmetry phase outside the heated bubble. It might thus be the interface between the hot bubble (with a maximum radius $R_b \sim 30$ μm) and the bulk superfluid outside which governs vortex formation.

Experiment.—The measurements are performed in a rotating nuclear demagnetization cryostat. The sample container is a quartz cylinder of radius $R = 2.5$ mm and height $L = 7$ mm [7]. While the sample is maintained at constant conditions, it is irradiated with paraffin moderated neutrons from a weak Am-Be source, to heat the fluid locally with the nuclear reaction $n + {}^3_2\mathrm{He} \rightarrow p + {}^3_1\mathrm{H} + 764$ keV. The distance of the source from the sample is adjusted such that the observed absorption reactions are well separated in time. At constant neutron flux we record the NMR absorption as a function of time. The height of a sudden jump in the NMR absorption measures the number of new vortex lines which are formed in a neutron absorption event. Because of the large absorption cross section

of the $^3_2$He nucleus, the mean free path of thermal neutrons in liquid ^{3}He is about 0.1 mm. Most reactions occur thus within a short distance from the side wall of the cylinder. Here the superflow velocity is $v_s = \Omega R$ with respect to the wall, when the cylinder is rotated in the vortex-free state at an angular velocity Ω [8]. When a vortex line is formed v_s decreases. The reduction is taken into account as described in Ref. [7]. In the worst case the measuring accuracy is $\Delta v_s \approx \pm 0.04$ mm/s.

Pressure dependence.—Vortex lines are detected only if the superflow velocity exceeds a threshold $v_{cn}(T, P, H)$, which is plotted as a function of pressure P and magnetic field H in Fig. 1. Experimentally v_{cn} is a well-defined quantity which estimates the effective radius R_b of the heated bubble: The largest vortex ring, which fits into the bubble, has a diameter $\mathcal{D} = 2R_b$. If the flow exceeds $v_s = v_{cn} \sim (\kappa/2\pi\mathcal{D}) \ln(\mathcal{D}/\xi)$, where $\kappa = h/2m$ is the circulation quantum and $\xi(T, P) \approx \xi_0(P)(1 - T/T_c)^{-1/2}$ the coherence length, a ring, with the correct sign of circulation and oriented perpendicular to the flow, expands into the bulk liquid. The pressure dependence in Fig. 1 displays an abrupt increase at about 21.2 bars, the pressure $P_{\rm PCP}$ of the polycritical point: Above $P_{\rm PCP}$ ^{3}He-A is stable in zero field below T_c between the normal and B phases. Thus, although the measurements in Fig. 1 are carried out well in the B phase, vortex formation is reduced when the quench trajectory crosses the stable A-phase regime [trajectory (a) in the inset of Fig. 1].

Magnetic field dependence.—The parabolic dependence of v_{cn} on the applied field H in Fig. 1 supports the same conclusion. The only major influence of small fields on a quench at low pressures [trajectory (b) in the inset of Fig. 1] is to make ^{3}He-A stable in a narrow interval from T_c down to the first order $A \rightarrow B$ transition at $T_{AB}(P, H)$. The magnetic field lowers the A-phase energy minimum with respect to that of the B phase and again this translates to a reduced yield of vortex lines at any given value of the bias v_s.

Consequences.—The results in Fig. 1 support the KZ mechanism and allow us to exclude other explanations. The most compelling of these is the superflow instability at the warm boundary of the heated bubble, where the liquid is still in B phase. This instability occurs at the ^{3}He-B pair-breaking velocity $v_c(T, P) \approx v_{c0}(P)(1 - T/T_c)^{1/2}$, where $v_{c0}(P) = 1.61(1 + F_1^s/3)k_{\rm B}T_c/p_{\rm F}$ [7]. In the bulk liquid $v_s \ll v_c$, but at the warm bubble boundary v_c is necessarily exceeded. However, v_{cn} in Fig. 1 does not follow the smooth pressure dependence of $v_{c0}(P)$. Together with the field dependence of v_{cn}, this suggests that it is not the boundary condition, but the interior of the heated bubble, which determines v_{cn}. This is understandable since the KZ mechanism should inherently be orders of magnitude faster than the hydrodynamic process for creating a large vortex ring with radius R_b.

The KZ interpretation for Fig. 1 is the following: During cool down through T_c the order parameter may

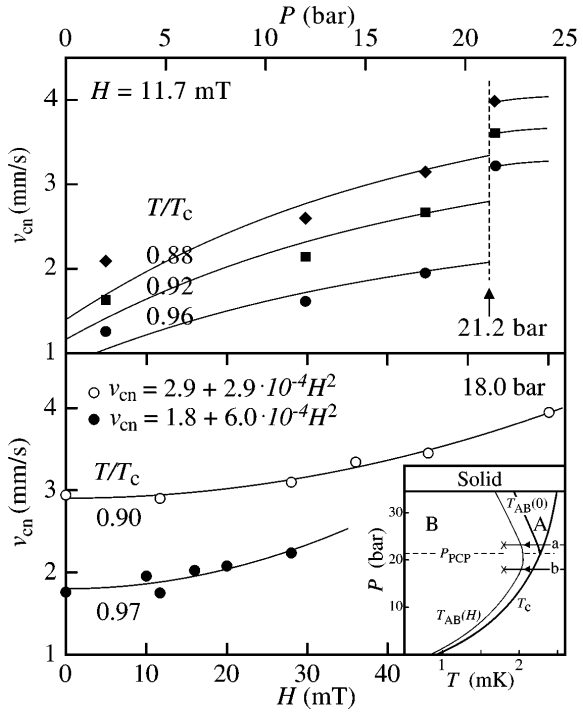

FIG. 1. Threshold velocity v_{cn} for the onset of vortex formation in neutron-irradiated ^{3}He-B superflow: (Top) The pressure dependence displays a steep change at $P_{\rm PCP}$ (although the B-phase properties are changing smoothly as a function of pressure). At $P < P_{\rm PCP}$, the curves represent $v_{cn} = (\epsilon\kappa/4\pi R_b)\ln(R_b/\xi)$, where $R_b = (3/2e\pi)^{1/2}(E_0/C_v T_c)^{1/3}(1 - T/T_c)^{-1/3}$ is obtained from the spherical thermal model with all of $E_0 = 764$ keV transformed to heat. The fitted scaling factor is $\epsilon = 2.1$. (Bottom) The dependence on the magnetic field is parabolic and reminiscent of the equilibrium state $A \rightarrow B$ transition $T_{AB}(P, H) = T_c(P)(1 - \alpha H^2)$, where $\alpha(P) \sim (0.5 - 10) \times 10^{-6}$ (mT)$^{-2}$ [14]. (Inset) Phase diagram of ^{3}He superfluids with superfluid transition at T_c, $A \rightarrow B$ transition at $T_{AB}(0)$ in zero and at $T_{AB}(H)$ in nonzero field, and two quench trajectories (a) and (b).

settle in different regions into A- or B-phase local free-energy minima. Blobs of size ξ_v of A and B phase are formed. Their relative number depends on the difference between the A- and B-phase energies. In ambient conditions, where only B phase is stable, the A-phase blobs shrink away. However, here the AB interface appears as an additional defect, which is formed where the A- and B-phase blobs meet. It is known from experiments with a moving AB interface that the penetration of vortex lines through the phase boundary is suppressed [9]. Thus we expect that A-phase blobs reduce the volume of the initial vortex network, which is confined within the B-phase blobs, and that vortex formation is impeded.

Figure 1 suggests two conclusions: (1) The KZ mechanism is the fastest process to create defects, before others become effective. Even in an inhomogeneous initial state with large thermal gradients, we may assume that the KZ mechanism dominates defect formation [10], if the velocity at which the phase front moves through the heated bubble, $v_T \sim R_b/\tau_Q \sim 6$ m/s, is comparable

to the critical value $v_{Tc} \sim v_F\,(\tau_0/\tau_Q)^{1/4}$. (2) In supercooled ^{3}He-A the KZ mechanism starts with finite probability the $A \rightarrow B$ transition. Suppose the initial state is supercooled ^{3}He-A in ionizing radiation. The final state is then the stable ^{3}He-B, although the boundary condition favors ^{3}He-A. The deeper the supercooling, the larger the proportion of B-phase blobs formed in the quench, and the more likely it is that some of them merge to a bubble which exceeds the critical diameter and starts the $A \rightarrow B$ transition, as is observed [11]. This explanation [12] does not require (or exclude) [13] Leggett's inverted "baked Alaska" temperature distribution within the heated bubble [11].

Velocity dependence.—Measurements of vortex-line formation as a function of the applied superflow velocity v_s allow a quantitative comparison to the KZ theory. In Fig. 2 we have counted per unit time the total number of vortex lines $\dot{N}_r$ (top), the number of those neutron absorption events $\dot{N}_e$ which produce at least one line (middle), and the number of lines extracted from each absorption event (bottom). The rates increase rapidly with v_s: At $v_s/v_{cn} \approx 4.5$, close to the maximum velocity limit imposed by the spontaneous nucleation threshold [7], there are almost no unsuccessful (and unobserved) absorption events left: $\dot{N}_e(\infty) - \dot{N}_e(4.5v_{cn}) \approx 0$. The data also display a universality property: The fitted expressions are of the form $\dot{N}_r = \gamma[(v_s/v_{cn})^3 - 1]$, where $v_{cn}(T, P, H)$ carries all dependence on the experimental variables. A number of tests showed no background contribution in the absence of the neutron source.

The most detailed information is the dispersion into events in which a given number of lines is formed. In Fig. 3 we plot the rates $\dot{N}_{ri}$ of events which produce up to $i = 5$ lines. These data display large statistical variation, but after averaging we get a curve for each value of i, which is shifted to successively higher velocities, peaks at a maximum, and then trails off. The curves start from a threshold velocity v_{cni}, plotted in the inset. At and immediately above $v_{cn} = v_{cn1}$ only single-vortex events occur. This means that the heated bubble resembles in shape more a sphere than a narrow cigar which is randomly oriented with respect to the flow.

Simulation.—The initial distribution of loops in a random vortex network with intervortex distance $\tilde{\xi} = \xi_v$

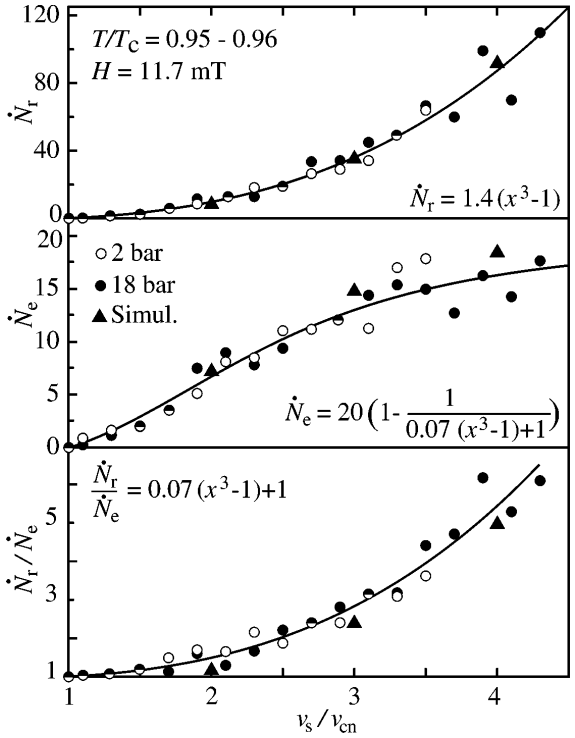

FIG. 2. Rates of vortex line formation vs normalized superflow velocity $x = v_s/v_{cn}$: (Top) Number of lines $\dot{N}_r$ and (middle) neutron absorption events $\dot{N}_e$ per minute; (bottom) number of lines per event ($\approx \dot{N}_r/\dot{N}_e$). All three rates have been determined *independently* from discontinuities in the NMR absorption. The solid curves are independent fits to the data, given by the expressions in each panel.

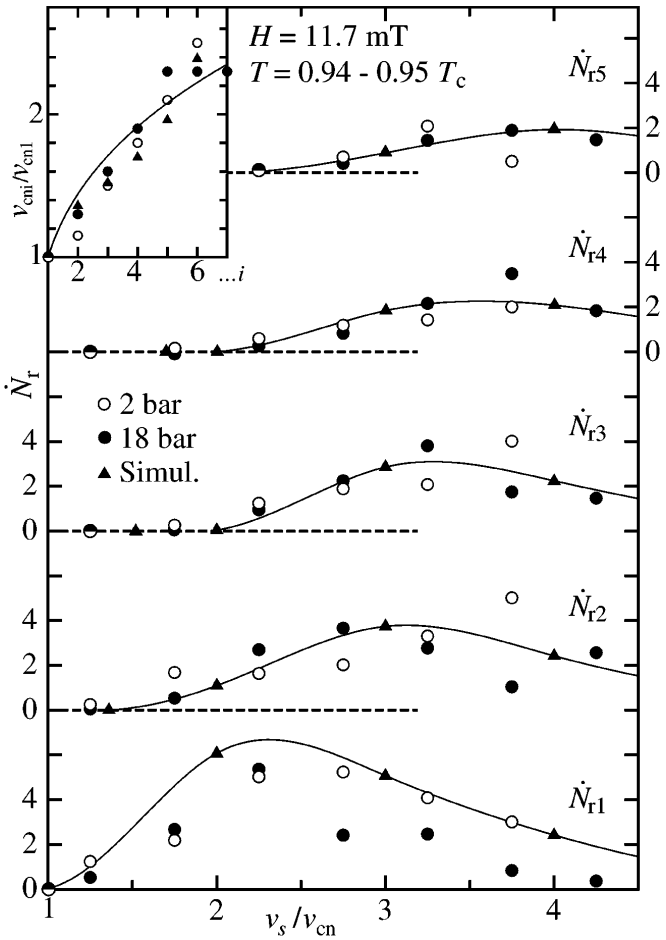

FIG. 3. Rates $\dot{N}_{ri}$ of vortex line formation, grouped according to the number of lines i formed per absorption event per minute, plotted vs v_s/v_{cn}. The solid curves are spline fits to the simulation data. (Inset) Threshold velocity v_{cni}/v_{cn1} for the onset of an event with i lines, plotted vs the number of lines i. The solid curve represents the fit $v_{cni}/v_{cn1} = [2.0(i - 1) + 1]^{1/3}$.

can be established with a standard simulation calculation [4,15]. We use a "cubic bubble" which is subdivided into a grid of unit size $\tilde{\xi}$, with up to 200^3 vertices. A random phase is assigned to each vertex initially, to model the randomly inhomogeneous order parameter. On the boundary of the bubble the phase is fixed, to ensure that no open-ended loops are formed. The results have been checked by averaging over up to 1000 different initial configurations. We use a continuous phase variable rather than restricting it to some set of allowed values. The distribution of the phase is extended to the edges of the grid according to the shortest path on the phase circle. Line defects are positioned to cross through the center of those grid faces for which the phase winding is nonzero.

As usual, we assume that the initial loop distribution is preserved during the later evolution [15], when the average intervortex distance $\tilde{\xi}(t)$ increases, but the network remains scale invariant, independently of the momentary value of $\tilde{\xi}(t)$. This property we use below when considering the escape of loops from the network. Two scaling relations of standard form hold for the networks:

$$n(l) = Cl^{-\beta} \ (C \approx 0.29,\ \beta \approx 2.3)\,, \tag{1}$$

$$\mathcal{D}(l) = Al^{\delta} \ (A \approx 0.93,\ \delta \approx 0.47)\,, \tag{2}$$

where we put $\tilde{\xi} = 1$, l and $\mathcal{D}$ are the length and average straight size diameter, and $n(l)$ the density of loops with length l. The numerical values of the parameters depend slightly on the size of the bubble, due to boundary conditions, but in the limit of a large bubble they are close to those obtained for networks with mostly open-ended strings [4,15]. For a Brownian random walk in infinite space the values of β and δ are $5/2$ and $1/2$.

Vortex loop escape.—The energy of a loop is given by

$$E(l, S, t) = \rho_s \kappa \left[l\, \frac{\kappa}{4\pi} \ln \frac{\tilde{\xi}(t)}{\xi} - v_s S \right], \tag{3}$$

where S is the algebraic area of the loop in the plane perpendicular to the direction of the superflow at v_s. A new result from our simulation is a scaling law for S:

$$|S| = B\mathcal{D}^{2-\nu} \ (B \approx 0.14,\ \nu \approx 0)\,. \tag{4}$$

Using Eq. (2) for $l(\mathcal{D})$ one has for a loop with $S > 0$

$$E(\mathcal{D}, t) = \rho_s \kappa \mathcal{D}^2 \left[\frac{\kappa}{4\pi \tilde{\xi}(t) A^2} \ln \frac{\tilde{\xi}(t)}{\xi} - v_s B \right]. \tag{5}$$

When the mean diameter of curvature $\tilde{\xi}(t)$ exceeds the critical value, $\tilde{\xi}_c(v_s) = (1/A^2 B)(\kappa/4\pi v_s) \ln \frac{\tilde{\xi}_c}{\xi}$, the energy becomes negative. Analytically the number of loops extracted per neutron is obtained from $N_r = V_b \int_{\tilde{\xi}_c}^{2R_b} d\mathcal{D}\, n(\mathcal{D})$, where $\tilde{\xi}_c(v_s = v_{cn}) = 2R_b$ defines the threshold velocity. This result is only a function of the relative velocity $x = v_s/v_{cn}$ and reproduces the measured dependence in Fig. 2: $N_r \propto x^3 - 1$. An event with i rings becomes possible, when $N_r \sim i$. This gives for its threshold velocity $v_{cni}/v_{cn} \sim i^{1/3}$, as measured in Fig. 3.

In the simulation we assume that each sufficiently large loop with $S > 0$ will escape and produce as many observed vortices as the length of its projection in the plane perpendicular to $\mathbf{v}_s$ divided by the length of the critical (smallest) ring. This is checked for different values of the applied velocity v_s. Results are plotted in Figs. 2 and 3.

The scaling calculation is justified in so far that the later evolution of the network is orders of magnitude slower than τ_Q. The latter has to be described separately with a calculation of the vortex dynamics [16], including mutual friction and the polarization of the vortex tangle by the superflow. We have performed preliminary calculations on small lattices (up to $40 \times 40 \times 40$) and find that even close to T_c the scaling law (1) remains valid at larger loop lengths $l > 4\tilde{\xi}$ and that the result for $\dot{N}_r(v_s/v_{cn})$ does not change qualitatively.

Conclusion.—We have established quantitative agreement between measurement and the KZ mechanism. It appears to be the fastest process by which a random network of defects is formed, before other phenomena, such as the superflow instability at the boundary of the heated bubble or superfluid turbulence within its interior, have a change to develop. A bias field of sufficient magnitude will select the type of defect, which remains stable while others relax. In superflow these are vortex loops. In supercooled ^{3}He-A it is blobs of ^{3}He-B, which have a finite probability to start the $A \rightarrow B$ transition.

*Permanent address: Kapitza Institute for Physical Problems, 117334 Moscow.
†Permanent address: Landau Institute for Theoretical Physics, 117334, Moscow.

[1] T. W. Kibble, J. Phys. A **9**, 1387 (1976).
[2] W. H. Zurek, Nature (London) **317**, 505 (1985); Phys. Rep. **276**, 177 (1996).
[3] V. M. Ruutu *et al.*, Nature (London) **382**, 334 (1996); C. Bäuerle *et al.*, Nature (London) **382**, 332 (1996).
[4] See eg., M. Hindmarsh and T. Kibble, Rep. Prog. Phys. **58**, 477 (1995); A. Bray, Adv. Phys. **43**, 357 (1994).
[5] I. Chuang *et al.*, Science **251**, 1336 (1991); M. J. Bowick *et al.*, Science **263**, 943 (1994).
[6] P. C. Hendry *et al.*, Nature (London) **368**, 315 (1994).
[7] Ü. Parts *et al.*, Europhys. Lett. **31**, 449 (1995).
[8] The proper variable in Figs. 2 and 3 is the counterflow velocity $v_{cf} = v_n - v_s$ and *not* $v_n = \Omega r$ [7].
[9] Ü. Parts *et al.*, Physica (Amsterdam) **197B**, 376 (1994).
[10] T. Kibble and G. Volovik, JETP Lett. **65**, 102 (1997).
[11] P. Schiffer, D. Osheroff, and A. Leggett, in *Progress in Low Temperature Physics* (Elsevier, Amsterdam, 1995), Vol. XIV, p. 159, and references therein.
[12] G. Volovik, Czech. J. Phys. **46**-Suppl. S6, 3048 (1996).
[13] Yu. Bunkov and O. Timofeevskaya, Report No. cond-mat/9706004 (to be published).
[14] Y. Tang *et al.*, Phys. Rev. Lett. **67**, 1775 (1991).
[15] T. Vachaspati and A. Vilenkin, Phys. Rev. D **30**, 2036 (1984).
[16] K. W. Schwarz, Phys. Rev. B **38**, 2398 (1988).